

## Notion d' « ondes de matière »

L'objectif de cette approche documentaire est d'étudier une expérience d'interférences entre objets matériels à l'aide d'un dispositif de type fentes d'Young.

### Article : Shimizu et al 1992

#### Double-slit interference with ultracold metastable neon atoms

Physical Review A

Volume 46, number 1

1 July 1992

Fujio Shimizu

*Department of Applied Physics, University of Tokyo, Bunkyo-ku, Tokyo 113, Japan*

Kazuko Shimizu and Hiroshi Takuma

*Institute for Laser Science, University of Electro-Communications, Chofu-shi, Tokyo 113, Japan*

(Received 16 December 1991; revised manuscript received 16 March 1992)

A double-slit interference of ultracold neon atoms in the  $1s_3$  metastable state is studied. The interferometer is aligned vertically, and because of gravity acceleration the atom changes its velocity as much as 2 m/s during the passage of the interference. The interference fringes are observed for the initial atomic velocity between 0 and 2 m/s.

PACS number(s) : 32.80.Pj, 07.60.Ly

The atomic interferometer is expected to have an extremely high phase sensitivity on rotation and acceleration of the apparatus. It is also very sensitive to the perturbation of potential energy along the atomic path in the interferometer. Interferometric effects of neutral atoms were first observed in diffracted device [1-4]. Recently, atomic interferometers that explicitly use beam splitting and recombining mechanisms were demonstrated with the Young's double-slit configuration [5], with gratings [6] and with a coherent transition between two internal states [7-9]. Although most of the works were done with atoms at room temperature, Kasevich and Chu [8] used laser-cooled Na atoms. Laser cooling can extend the range of application of atomic interferometers. A long de Broglie wavelength of the laser-cooled atom reduces the accuracy requirement of components by several orders of magnitude. A slow atomic beam can easily be deflected by a large angle with electromagnetic and optical dipole forces. Therefore, an atomic interferometer with a dimension similar to an optical interferometer may be constructed. In a cold-atom interferometer the atom takes a long time to move through. This increases drastically the phase sensitivity against the perturbation of potential energy.

The difficulty in constructing a cold-atom interferometer arises because the atomic beam flux decreases rapidly with atomic velocity. The beam splitting by a coherent transition of atomic internal states reduces this problem, because all atoms illuminated by the resonant light can contribute to the interference regardless of their position. In the experiment by Kasevich and Chu [8], they used a coherent Raman transition between the ground-state hyperfine doublet. To construct a spatially fixed interferometer, however, the luminosity of the atomic beam has to be improved. This article describes the revised work of our preliminary report on double-slit interference with laser-cooled singlet atoms [10]. In our double-slit interferometer, we use an optically generated atomic point source in place of the collimating slit. This technique increases the luminosity of the beam, because atoms trapped in a large volume are funneled into a narrow transfer beam. Furthermore, the atomic state can be converted to one which is favorable for

the cooled-atom interferometer. As a result we obtained a two-dimensional interference pattern at various atomic velocities in a single experiment run. The result was almost background free and was capable of the quantitative analysis even though the interference time was as long as 0.2 s. The improvement is clear if one compares with the first double-slit experiment by Carnal and Mlynek [5] with a conventional collimation method and with atoms at room temperature, in which they could obtain only one-dimensional information.

Our atomic source is  $1s_3$  metastable neon atoms, which are generated by focusing a 598-nm laser beam into a magneto-optical trap [11] containing  $1s_5$  metastable neon atoms [12]. The 598-nm laser excites the  $1s_5$  atoms to the  $2p_5$  state. Approximately one half of the  $2p_5$  population decays to the  $1s_3$  ( $J = 0$ ) metastable state with an approximate decay time of 20 ns [13]. The rest decays to the ground state through  $1s_1$  or  $1s_4$  state by emitting 75-nm vuv photons. Since the  $1s_3$  atoms are not influenced by the 640-nm trapping laser or the magnetic field, their trajectory is determined only by the initial velocity and gravity. The velocity change during the  $1s_5$  to  $1s_3$  conversion process is at most 5 cm/s. Therefore, the initial velocity distribution of the  $1s_3$  atoms is practically the same as that of the trapped  $1s_5$  atoms. The size of the  $1s_3$  atomic source is much larger than the size of the beam source used in the interferometer with thermal atoms [5, 6]. This is tolerated for laser-cooled atoms, because the de Broglie wavelength is 3 orders of magnitude longer than the case of a thermal beam. Other advantages for use of the  $1s_3$  metastable neon are that the  $1s_3$  state has no level multiplicity, which complicates the manipulation of atomic beam, and that they are easily detected by a high sensitive detector such as an electron multiplier or a microchannel plate detector (MCP).

Figure 1 shows the experimental setup. The  $1s_3$  metastable neon atoms were trapped in a magneto-optical trap using four laser beams [14]. The size of the cloud of atoms in the trap was typically 1 mm in diameter. A 598-nm laser which pumped the  $1s_5$  atom to the  $2p_5$  state was introduced through a single-mode optical fiber from the top of the trap chamber. The exit of the optical fiber was imaged in the middle of the trap using a  $f =$

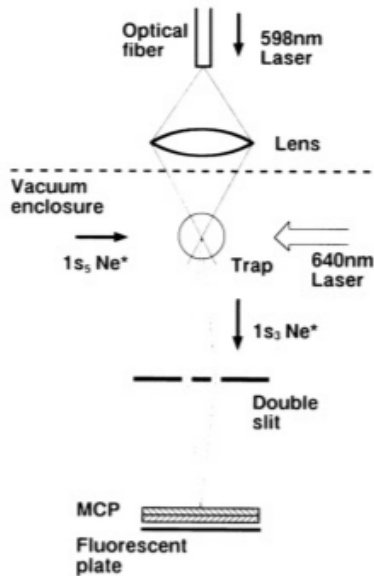


FIG. 1. Schematic experimental configuration. Details of the trap are not shown.

55-mm camera lens with the magnification of 4. A half-maximum diameter of the laser at the focus was  $200 \mu\text{m}$ , and at the  $1/10$  intensity the diameter increased to  $80 \mu\text{m}$ . The depth of the focus was approximately  $1 \text{ mm}$ . The temperature of the trapped atoms was approximately  $2.5 \text{ mK}$ . The  $1s_3$  atoms generated in the trap started to fall, passed through a double slit placed  $76 \text{ mm}$  below the trap and hit a two stage MCP equipped with a fluorescent plate placed a further  $113 \text{ mm}$  below. The double slit had the opening of  $2 \mu\text{m}$  width separated by  $6 \mu\text{m}$  (center to center). The  $1s_3$  metastable source and the slit were aligned vertically along the direction of the gravity within  $1/200$  radian. To reject electrons hitting the MCP the potential of the first surface was kept at  $-40\text{V}$  relative to the vacuum chamber. The MCP displayed spots of individual metastable atoms, positive neon ions, or  $75\text{-nm}$  vuv photons. The spot size was typically  $80 \mu\text{m}$ . The image was amplified by a charge coupled device (CCD) camera and recorded on a videotape.

The timing of the operation was synchronized to the vertical synchronizing signal of the CCD camera. The camera was operated by the "field" mode which had the temporal resolution of  $1/60 \text{ s}$ . The cooling  $640\text{-nm}$  laser was on for four field lengths ( $4/60 \text{ s}$ ). The trap grew with the time constant of typically  $10 \text{ ms}$ . The pumping laser at  $598 \text{ nm}$  was turned on  $2/60 \text{ s}$  after the turn-on of the cooling laser and was kept on for two field lengths. The intensity of the  $598\text{-nm}$  laser was adjusted so that  $50\%$  to  $60\%$  of the trapped  $1s_3$  atoms were transferred to the  $1s_3$  or ground state during this period. Then, both lasers were shut off for a period of twelve field lengths ( $1/5 \text{ s}$ ). The process was repeated with a time interval of  $16/60 \text{ s}$ . The recorded tape contained pictures of 16 different time intervals relative to the switching of the lasers. In the following description we choose the time origin to the middle of the illumination period of the  $598\text{-nm}$  laser, which was the average starting time of the  $1s_3$  atoms from the trap. To construct a picture of the interference pattern, the center of the gravity of all spots was calculated and accumulated for video frames of each time interval using a graphic processor. The resolution of the picture on the MCP was approximately  $20 \mu\text{m}$ , which was

determined by the pitch of the CCD element. When the  $640\text{-nm}$  laser was on, the trap released  $\text{Ne}^+$  which produced a broad background image of the slit on the recording. When the  $598\text{-nm}$  laser was on, spots of the  $75\text{-nm}$  vuv spontaneous photons were superimposed, which produced a distinctive interference pattern with a fringe separation of  $1.2 \text{ mm}$ . Spots due to the cold  $1s_3$  metastable atoms were recorded when both lasers were off, and the video frames at different time intervals showed the images generated only by atoms with different velocity. Typical  $1s_3$  and vuv counts available for the analysis were  $1.5$  and  $1.9 \text{ s}^{-1}$ , respectively. Figure 2 shows the interference pattern by the metastable atoms that arrived at the time between  $t = 0.158$  and  $0.225 \text{ s}$ . In this picture the velocity of the  $1s_3$  atoms at the source (trap)  $v_0$  was between  $42$  and  $-26 \text{ cm/s}$ . The atoms were accelerated to  $v_s = 1.25 \text{ m/s}$  on average at the slit, and the velocity on the MCP was  $v_d = 1.93 \text{ m/s}$ . The accumulation time was  $15/8 \text{ h}$  and the picture contains approximately  $6 \times 10^3$  spots. The interference pattern in the top half of the picture was somewhat smeared due to the damage of the double-slit structure. The bottom  $1/3$ , corresponding to the length of  $0.5 \text{ mm}$  on the slit, was used in the following analysis.

Assuming that the atom falls along the classical path, the phase difference of the atom which has fallen by the distance  $l$  as a function of the distance  $x$  from the vertical line passing through the source is

$$\Delta\phi = \frac{mv_s}{\hbar} \frac{x^2}{2l} \frac{\alpha}{2(\sqrt{1+\alpha}-1)}, \quad (1)$$

where  $\alpha = 2gl/v_s^2$ ,  $v_s$  is the velocity of the atom at the top,  $m$  the mass of the atom, and  $g$  the gravitational acceleration. Therefore, the fringe separation  $\Delta x$  is given by

$$\Delta x = \frac{h}{mv_s} \frac{l}{d} \frac{2(\sqrt{1+\alpha}-1)}{\alpha}, \quad (2)$$

where  $d$  is the separation of the double slit and  $l$  the distance between the slit and the MCP. Since  $h/mv_s$  is the de Broglie wavelength of the atom at the slit, this expression is the same as the optical case, except for the factor which arises from the acceleration by the gravity during the fall.

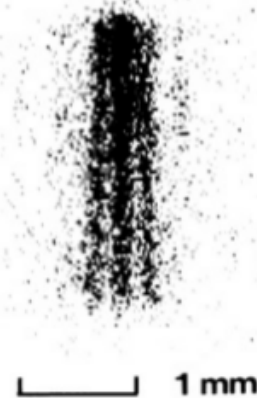


FIG. 2. The interference fringe pattern on the MCP for atoms with the initial velocity of approximately zero. The vertical length of the slit image is  $2.8 \text{ mm}$ . The spatial resolution of the picture is  $20$  and  $32 \mu\text{m}$  for the horizontal and vertical directions, respectively. The narrowing of the fringe separation on the upper part is due to the damage of the double-slit structure. This figure contains approximately  $6 \times 10^3$  atomic counts.

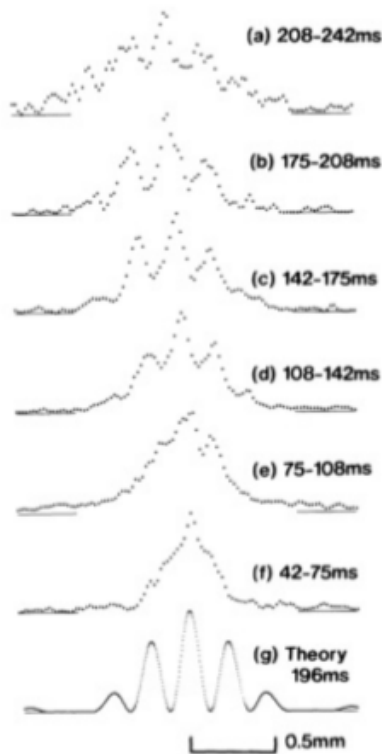


FIG. 3. (a)–(f) The interference pattern vs the transit time  $t$  of the  $1s_3$  atom from the trap to the MCP. (g) The calculated pattern for  $v_0 = 0$  m/s.

Figure 3 shows the intensity profile perpendicular to the slit direction of the video frames at (a)  $t = 225$ , (b) 192, (c) 158, (d) 125, (e) 92 and (f) 58 ms. These curves were averaged among successive 3 data points in the figure with the weighting ratio of 1:2:1 to reduce a large point-to-point fluctuation. Figure 3(g) is the theoretical curve for the atom with zero velocity at the source and  $t = 196$  ms approximately corresponding to the experimental curve of Fig. 3(b). The measured fringe separation was  $227 \mu\text{m}$ , which was in relatively good agreement with the calculated value of  $238 \mu\text{m}$  at  $v_0 = 0$  m/s, considering that the slit used in this experiment has a problem in uniformity as evidenced from Fig. 2. The contrast ratio of the experimental fringe was somewhat reduced due to the finite size of the  $1s_3$

metastable source, to the velocity spread within one frame of the video recording, and to the slight misalignment of the vertical line which caused the velocity dependent shift of the fringe position. In Fig. 3(a) atoms moved first upwards before they started to fall towards the slit. In this figure the 640-nm cooling laser was on and the  $\text{Ne}^+$  ions generated by collisions between trapped  $1s_3$  neon atoms caused a large background. Figure 4 shows the variation of the interference fringe separation against the arrival time of the metastable atoms. The value agrees quite well with the theoretical value calculated from Eq. (2), which is drawn by a solid line.

In conclusion we have demonstrated double-slit interference of extremely cold atoms that were constantly accelerated by gravity and whose translational wave function was largely different from the free-space wave function. The long interaction time of this interferometer makes it a very sensitive device for the measurement of potential variation and acceleration. The low atomic count rate of the present system can be improved by using a transversely collimated ultracold monoenergetic atomic beam, instead of the trap. It is also possible to increase the atomic flux by collimation using a static or microwave electric field.

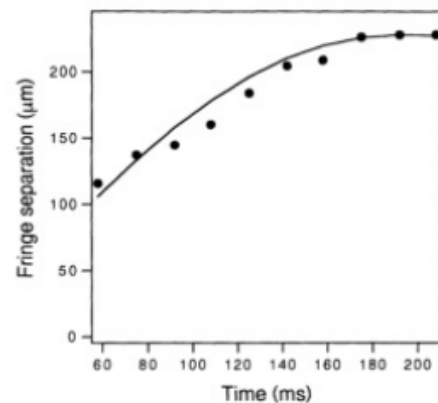


FIG. 4. The fringe separation vs the transit time. The solid line is calculated from Eq. (2).

[1] I. Estermann and O. Stern, *Z. Phys.* 61, 95 (1930).  
 [2] D. W. Keith, M. L. Shattenburg, H. I. Smith, and D. E. Pritchard, *Phys. Rev. Lett.* 61, 1580 (1988).  
 [3] A. Faulstich, O. Carnal and J. Mlynek, in *Light Induced Kinetic Effects on Atoms, Ions and Molecules*, edited by L. Moi, S. Gozzini, C. Gabbanini, E. Arimond, and F. Strumia (Ets Editrice, Pisa, 1991).  
 [4] P. L. Gould, G. A. Ruff, and D. E. Pritchard, *Phys. Rev. Lett.* 56, 827 (1986).  
 [5] O. Carnal and J. Mlynek, *Phys. Rev. Lett.* 66, 2689 (1991).  
 [6] D. W. Keith, C. R. Ekstrom, Q. A. Turchette, and D. E. Pritchard, *Phys. Rev. Lett.* 66, 2693 (1991).  
 [7] F. Riehle, Th. Kisters, A. Witte, J. Helmcke, and Ch. J. Borde, *Phys. Rev. Lett.* 67, 177 (1991).  
 [8] M. Kasevich and S. Chu, *Phys. Rev. Lett.* 67, 181 (1991).

[9] Ch. Miniatura, F. Perales, G. Vassilev, J. Reinhardt, J. Robert and J. Baudon, *J. Phys. II (France)* 1, 425 (1991).  
 [10] K. Shimizu, H. Takuma and F. Shimizu, in *Proceedings of the Tenth International Conference on Laser Spectroscopy*, edited by M. Ducloy, E. Giacobino, and G. Camy (World Scientific, Singapore, 1992).  
 [11] E. L. Raab, M. Prentiss, A. Cable, S. Chu, and D. E. Pritchard, *Phys. Rev. Lett.* 59, 2631 (1987).  
 [12] F. Shimizu, K. Shimizu, and H. Takuma, *Phys. Rev. A* 39, 2758 (1989).  
 [13] F. A. Sharpton, R. M. St. John, C-C. Lin, and F. E. Fajen, *Phys. Rev. A* 2, 1305 (1970).  
 [14] F. Shimizu, K. Shimizu, and T. Takuma, *Opt. Lett.* 16, 339 (1991).

## Questions

1. Quel est le but de cette expérience ?
2. Faire une description concise mais précise du dispositif expérimental. On précisera entre autres concernant les particules : la production, le piégeage, le refroidissement, le trajet, la détection.
3. Comparer ce dispositif avec celui des trous d'Young en optique. Comparer (similitudes et différences) l'expression de l'interfrange avec celle en optique.
4. Pourquoi les franges d'interférences ne sont-elles pas parallèles ici ?  
donnant la longueur d'onde associée à une particule en mécanique quantique en fonction de la constante de Planck  $h$  et de la quantité de mouvement de la particule  $p$ .
5. Pourquoi refroidit-on les atomes ? On s'appuiera sur la longueur d'onde de Broglie.
6. Application numériques :
  - Calculer la longueur d'onde de de Broglie dans cette expérience.
  - Calculer le coefficient  $\alpha$  du à la gravité contenu dans l'expression de l'interfrange.
  - Calculer l'interfrange  $\Delta x$ . Comparer à la valeur indiquée dans le texte et à l'ordre de grandeur indiqué par la figure 2.